

# Dual virtual element method in presence of an inclusion

Alessio Fumagalli

---

## Abstract

We consider a Darcy problem for saturated porous media written in dual formulation in presence of a fully immersed inclusion. The lowest order virtual element method is employed to derive the discrete approximation. In the present work we study the effect of cells with cuts on the numerical solution, able to geometrically handle in a more natural way the inclusion tips. The numerical results show the validity of the proposed approach.

*Keywords:* VEM, Darcy flow, fractured porous media, inclusion

---

## 1. Introduction

Single-phase flow in fractured porous media is a challenging problem involving different aspects, *i.e.* the derivation of proper mathematical models to describe fracture surrounding porous media flow and the subsequent discretization with ad-hoc numerical schemes. One of the most common approach is to consider fractures as co-dimensional objects and derive proper reduced models and coupling condition to describe the flow in the new setting. A hybrid dimensional description of the problem is thus introduced, see [1–5]. In presence of multiple fractures, forming a complex system of network, grid creation may become challenging and the number of cells or their shape may not be satisfactory for complex application, *e.g.*, the benchmark study proposed in [6].

In the present work we simplify the problem considering a single fracture and substituting with an inclusion, *i.e.* the flow problem in the fracture is not considered but its effect of its normal flow. The inclusion is an internal condition for the problem. We consider two extreme cases: perfectly permeable fracture (infinite normal permeability) and impermeable fracture (zero normal permeability). The pressure imposed on both sides of the inclusion determines these two cases.

The virtual element method (VEM), introduced in [7–15], is able to discretize the problem on grids with rather general cell shape. The theory developed in the aforementioned works considers star shaped cells. In the present study, the lowest order VEM is considered in presence of cells with an internal cut for the approximation at the tips of the inclusion.

The paper is organised as follow. In Section 2 the mathematical model and its weak formulation are presented. Section 3 introduces the discrete formulation of the problem. Numerical examples are reported in Section 4 for both the extreme cases. The work finishes with conclusions Section 5.

## 2. Mathematical model

Let us set  $\Omega \subset \mathbb{R}^2$  a regular domain representing a saturated porous media. We consider the Darcy model for single phase flow in a saturated porous media written in dual formulation, namely

$$\mathbf{u} + K\nabla p = \mathbf{0} \text{ in } \Omega \quad \wedge \quad \nabla \cdot \mathbf{u} = f \text{ in } \Omega \quad \wedge \quad p = 0 \text{ on } \partial\Omega. \quad (1a)$$

The unknowns are:  $\mathbf{u}$  the Darcy velocity and  $p$  the fluid pressure. In (1a)  $K$  represents the permeability matrix, symmetric and positive defined, and  $f$  a scalar source or sink term. To keep the presentation simple we consider only homogeneous boundary condition for the pressure at the outer boundary of  $\Omega$ , denoted by  $\partial\Omega$ . Coupled to (1a) we are interested to model an immersed inclusion  $\gamma$ , see Figure 1 as an example. With an abuse of notation,  $\partial\Omega$  does not include  $\gamma$  which represents an internal boundary for  $\Omega$ . It is possible to define a unique normal  $\mathbf{n}$  associated to  $\gamma$  and

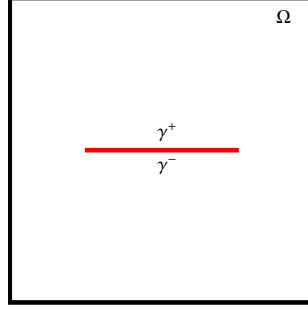


Figure 1: domain

two different sides of  $\gamma$  with respect to the direction of  $\mathbf{n}$ . We indicate them as  $\gamma^+$  and  $\gamma^-$ , with  $\mathbf{n}^+ = \mathbf{n}$  and  $\mathbf{n}^- = -\mathbf{n}$  the associated normals. It is important to note that geometrically  $\gamma$ ,  $\gamma^+$ , and  $\gamma^-$  are indeed the same object but introducing the two sides help us to impose different internal conditions. We have

$$p = p^+ \text{ on } \gamma^+ \quad \wedge \quad p = p^- \text{ on } \gamma^-. \quad (1b)$$

We define the Hilbert spaces  $Q = L^2(\Omega)$  and  $V = H_{\text{div}}(\Omega)$ . By standard arguments the weak formulation of (1) reads

$$a(\mathbf{u}, \mathbf{v}) + b(\mathbf{v}, p) = J(\mathbf{v}) \quad \forall \mathbf{v} \in V \quad \wedge \quad b(\mathbf{u}, q) = F(q) \quad \forall q \in Q. \quad (2)$$

In 2 we have indicated by  $(\cdot, \cdot)_\Omega$ :  $Q \times Q \rightarrow \mathbb{R}$  the scalar product in  $Q$ . The bilinear forms and functionals are defined as

$$\begin{aligned} a(\cdot, \cdot) : V \times V \rightarrow \mathbb{R} \quad \text{s.t.} \quad a(\mathbf{w}, \mathbf{v}) &:= (K^{-1}\mathbf{w}, \mathbf{v})_\Omega, & b(\cdot, \cdot) : V \times Q \rightarrow \mathbb{R} \quad \text{s.t.} \quad b(\mathbf{v}, q) &:= -(\nabla \cdot \mathbf{v}, q)_\Omega, \\ J(\cdot) : V \rightarrow \mathbb{R} \quad \text{s.t.} \quad J(\mathbf{v}) &:= -\langle \mathbf{v}^+ \cdot \mathbf{n}^+, p^+ \rangle_{\gamma^+} - \langle \mathbf{v}^- \cdot \mathbf{n}^-, p^- \rangle_{\gamma^-}, & F(\cdot) : Q \rightarrow \mathbb{R} \quad \text{s.t.} \quad F(q) &:= -(f, q)_\Omega \end{aligned}$$

where the duality pairings are defined as  $\langle \cdot, \cdot \rangle_{\gamma^\pm} : H^{-\frac{1}{2}}(\gamma^\pm) \times H^{\frac{1}{2}}(\gamma^\pm) \rightarrow \mathbb{R}$ . We are assuming  $p^\pm \in H^{\frac{1}{2}}(\gamma^\pm)$  and  $f \in L^2(\Omega)$ . Following [15] problem (2) is well posed.

### 3. Discrete formulation

The creation of a computational grid with multiple intersecting inclusions, or more generally fractures, is a challenging aspect possibly resulting in a high number and/or poorly shaped cells. To overcome this aspect we consider a VEM formulation with a clustering technique from a finer triangular grid.

We consider now the discrete formulation of problem (2) employing the VEM. For simplicity we limit our analysis to the lowest order case. For a more general case we refer to [7–14]. Let be  $\mathcal{T}(\Omega)$  a generic tessellation of  $\Omega$  made of non-overlapping polytopes. We allow non-star shaped cells by considering cells with an internal cut. We introduce the following approximation spaces for  $p$  and  $\mathbf{u}$ . For a cell  $E \in \mathcal{T}(\Omega)$  with edges  $\mathcal{E}(E)$ , let us define

$$Q_h(E) := \{q \in Q : q \in \mathbb{P}_0(E)\} \quad \wedge \quad V_h(E) := \{\mathbf{v} \in V : \mathbf{v} \cdot \mathbf{n}|_e \in \mathbb{P}_0(e) \forall e \in \mathcal{E}(E), \nabla \cdot \mathbf{v} \in \mathbb{P}_0(E), \nabla \times \mathbf{v} = \mathbf{0}\}. \quad (3)$$

The norms and the global spaces,  $Q_h$  and  $V_h$ , are defined accordingly. With the definition (3) it is possible to compute immediately the discrete approximation of  $b(\cdot, \cdot)$ ,  $J(\cdot)$ , and  $F(\cdot)$ . Since the shape of the functions in  $V_h(E)$ , for each cell  $E \in \mathcal{T}(E)$ , is not prescribed we cannot compute directly the bilinear form  $a(\cdot, \cdot)$ . In this case we need to introduce a sub-space of  $V_h$  and a projection operator, the space is

$$\mathcal{V}_h(E) := \{\mathbf{v} \in V_h(E) : \mathbf{v} = \nabla v, \text{ for } v \in \mathbb{P}_1(E)\}$$

It is worth noting that the local approximation of  $\mathbb{P}_1(E)$  is done by means of a suitable monomial expansion. The projection operator is defined locally as  $\Pi_0 : V(E) \rightarrow \mathcal{V}_h(E)$  such that  $a(T_0 \mathbf{u}, \mathbf{v}) = 0$  for all  $\mathbf{v} \in \mathcal{V}_h(E)$ , with  $T_0 := I - \Pi_0$  the projection on the orthogonal space of  $\mathcal{V}_h$ . Considering the property of the projection operator, we make the following



Figure 2: Detail of the computational grids on the left tip of  $\gamma$ , depicted in red.

$h$	$err(p)$	$\mathcal{O}(h)$	$err(p)$	$\mathcal{O}(h)$
$7.942 \cdot 10^{-2}$	$3.045 \cdot 10^{-2}$	-	$2.266 \cdot 10^{-2}$	-
$3.801 \cdot 10^{-2}$	$1.545 \cdot 10^{-2}$	0.92	$1.217 \cdot 10^{-2}$	0.84
$1.920 \cdot 10^{-2}$	$8.03 \cdot 10^{-3}$	0.96	$5.916 \cdot 10^{-3}$	1.06
$9.692 \cdot 10^{-3}$	$1.830 \cdot 10^{-3}$	2.16	$2.913 \cdot 10^{-3}$	1.04

Table 1: On the left: (4) for example in Subsection 4.1. On the right: (4) for the example in Subsection 4.2.

approximation  $a(\mathbf{u}, \mathbf{v}) \approx a_h(\mathbf{u}, \mathbf{v}) := a(\Pi_0 \mathbf{u}, \Pi_0 \mathbf{v}) + s(T_0 \mathbf{u}, T_0 \mathbf{v})$ , where the first part is a consistency term and the second a stabilization term. The latter is approximated by the bilinear form  $s(\cdot, \cdot)$  such that an equivalence property holds true, *i.e.*  $\exists \iota_*, \iota^* \in \mathbb{R}$  independent from the discretization size  $h$  satisfying  $\iota_* a(\Pi_0 \mathbf{v}, \Pi_0 \mathbf{v}) \leq s(T_0 \mathbf{v}, T_0 \mathbf{v}) \leq \iota^* a(\Pi_0 \mathbf{v}, \Pi_0 \mathbf{v})$ , see the aforementioned work for more details. With these choices the bilinear form  $a_h(\cdot, \cdot)$  is computable for each cell of the grid.

#### 4. Numerical example

In this section we present a numerical study to investigate the error decay for the model presented previously. Two examples are shown with the same and different boundary conditions on the internal boundary  $\gamma$ . We consider the domain depicted in Figure 1 with  $\Omega = [0, 1]^2$  and  $\gamma = \{(x, y) : 0.25 \leq x \leq 0.75 \wedge y = 0.5\}$ .

The reference solution, named  $p_{\text{ref}}$ , is computed considering a grid of 77546 triangles very refined at the ending points of  $\gamma$ . The  $L^2$  relative error presented below is defined as

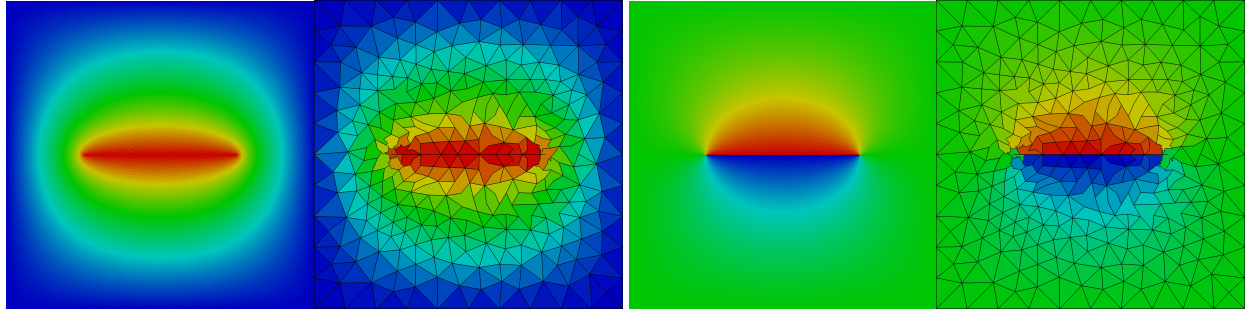
$$err(p) = \frac{\|p - p_{\text{ref}}\|_{L^2(\Omega)}}{|\max p_{\text{ref}} - \min p_{\text{ref}}|}. \quad (4)$$

In both cases we generate a family of triangular grids with a different level of refinement, in particular, close to the ending points of  $\gamma$ . Later, an agglomeration technique is employed based on the cell measure: neighbour cells with small measure are glue together forming new cells. To stress the method presented previously we enforce the creation, at the tips of  $\gamma$ , of cells with internal cuts. Figure 2 shows a zoom of the considered grids at the left ending point of  $\gamma$ . It is worth noting that the computation of the mesh size  $h$  is itself complex.

The implementation is done with PorePy: a simulation tool for fractured and deformable porous media written in Python. See [github.com/pmgbergen/porepy](https://github.com/pmgbergen/porepy) for further information. All the examples of this section are available in the package. In the following pictures a “Blue to Red Rainbow” colour map is used.

##### 4.1. Continuous pressure condition

We consider  $p^+ = p^- = 1$  as condition for  $\gamma^+$  and  $\gamma^-$ . The pressure solution of the reference and of the coarser grid is reported in Figure 3 on the left. We notice that the solution computed on the coarse grid with cells containing a cut resembles the reference solution, even at the tips of the inclusion. The error, computed for each cell of the reference grid, is represented in Figure 4. The error is distributed in the domain without any specific peak at the tips. In this case we can conclude that the cells with a cut do not deteriorate the quality of the solution. Finally, the error decay is given in Table 1 on the left confirming a first order of convergence.



(a) Reference and coarse solution for the continuous case.

(b) Reference and coarse solution for the discontinuous case.

Figure 3: On the left: pressure (range  $(0, 1)$ ) for the continuous case. On the right: pressure (range  $(-1, 1)$ ) for the discontinuous case.

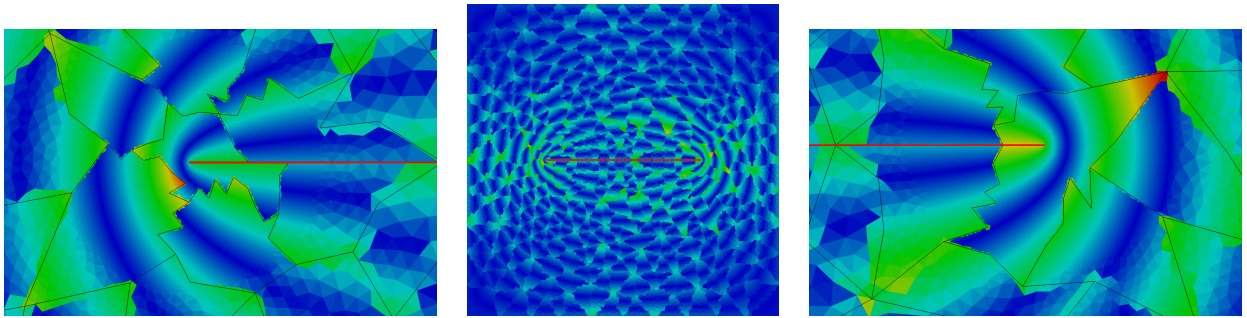


Figure 4: In the centre: the error on  $\Omega$  represented on the reference grid. On the right and left: a zoom of the error for the right and left tip, respectively. Range in  $(0, 0.25)$ .

#### 4.2. Discontinuous pressure condition

We consider  $p^+ = 1$  for  $\gamma^+$  and  $p^- = -1$  for  $\gamma^-$  as boundary condition for the inclusion. We expect a jump in the solution and a poor regularity at the tips of  $\gamma$ . The pressure solution of the reference and of a coarse grid is reported in Figure 3 on the right. The solution computed with the coarse grid is in accordance with the reference solution, even at the tips of the inclusion. The error, computed for each cell of the reference grid, is depicted in Figure 5. We point out that the error is focused at the tips of the inclusion, since a complex solution is now approximated with a single degree of freedom on each coarse cell containing the tip. Nevertheless, the errors listed in Table 1 confirm also in this case a first order of convergence, thus the quality of the computed solution.

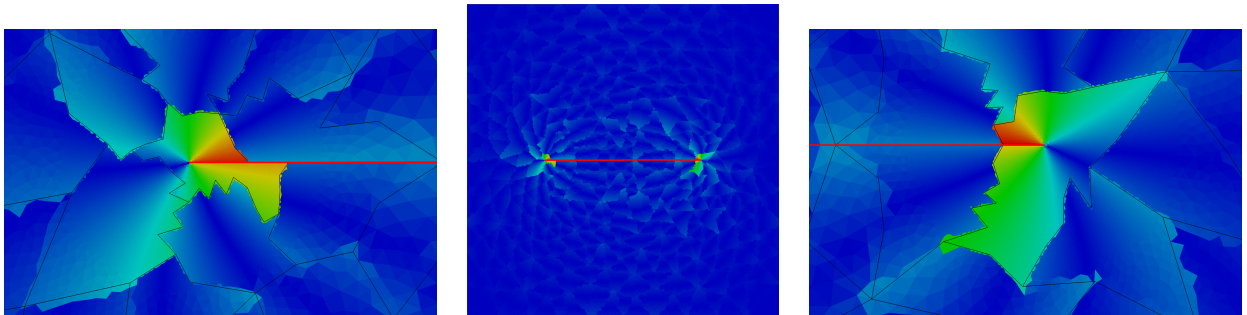


Figure 5: From the left: reference solution, coarse solution, and solution (range  $(0, 0.57)$ ) for the continuous case.

## 5. Conclusion

In this work we studied the applicability of a dual virtual element method in presence of cells with a cut for a problem with an inclusion. The proposed scheme behaved accurately obtaining correct results and error decay. For a different conditions at the inclusion a pick of error was concentrated at the inclusion tips, because a complex solution was approximated with a constant. However, the solution was not deteriorate and the global error was acceptable. While in the case of equal condition at the inclusion, a more uniform error was observed inside the domain. This is a promising approach to enlight the computational cost in presence of multiple inclusions, or even fractures represented as co-dimensional domains, which is currently under investigation.

## Acknowledgment

We acknowledge financial support for the ANIGMA project from the Research Council of Norway (project no. 244129/E20) through the ENERGIX program. The author wish to thank: Runar Berge, Inga Berre, Wietse Boon, Eirik Keilegavlen, and Ivar Stefansson for many fruitful discussions.

## Bibliography

### References

- [1] M. Karimi-Fard, L. J. Durlofsky, K. Aziz, An Efficient Discrete-Fracture Model Applicable for General-Purpose Reservoir Simulators, *SPE Journal* 9 (2) (2004) 227–236.
- [2] V. Martin, J. Jaffré, J. E. Roberts, Modeling Fractures and Barriers as Interfaces for Flow in Porous Media, *SIAM J. Sci. Comput.* 26 (5) (2005) 1667–1691. doi:10.1137/S1064827503429363.  
URL <http://scitation.aip.org/getabs/servlet/GetabsServlet?prog=normal&id=SJ0CE3000026000005001667000001&idtype=cvips&gifs=yes>
- [3] C. D’Angelo, A. Scotti, A mixed finite element method for Darcy flow in fractured porous media with non-matching grids, *Mathematical Modelling and Numerical Analysis* 46 (02) (2012) 465–489. doi:10.1051/m2an/2011148.
- [4] S. Berrone, S. Pieraccini, S. Scialò, A PDE-constrained optimization formulation for discrete fracture network flows, *SIAM Journal on Scientific Computing* 35 (2). doi:10.1137/120865884.
- [5] L. Formaggia, A. Fumagalli, A. Scotti, P. Ruffo, A reduced model for Darcy’s problem in networks of fractures, *ESAIM: Mathematical Modelling and Numerical Analysis* 48 (2014) 1089–1116. doi:10.1051/m2an/2013132.  
URL [http://www.esaim-m2an.org/article\\_S0764583X13001325](http://www.esaim-m2an.org/article_S0764583X13001325)
- [6] B. Flemisch, I. Berre, W. Boon, A. Fumagalli, N. Schwenck, A. Scotti, I. Stefansson, A. Tatomir, Benchmark of single-phase flow in fractured porous media with non-conforming discretization methods, Tech. rep., arXiv:1701.01496 [math.NA] (2017).  
URL <https://arxiv.org/abs/1701.01496>
- [7] L. Beirão da Veiga, F. Brezzi, D. L. Marini, Virtual elements for linear elasticity problems, *SIAM Journal on Numerical Analysis* 51 (2) (2013) 794–812. arXiv:<http://dx.doi.org/10.1137/120874746>, doi:10.1137/120874746.  
URL <http://dx.doi.org/10.1137/120874746>
- [8] L. Beirão da Veiga, F. Brezzi, L. D. Marini, A. Russo, The hitchhiker’s guide to the virtual element method, *Mathematical Models and Methods in Applied Sciences* 24 (08) (2014) 1541–1573. arXiv:<http://www.worldscientific.com/doi/pdf/10.1142/S021820251440003X>, doi:10.1142/S021820251440003X.  
URL <http://www.worldscientific.com/doi/abs/10.1142/S021820251440003X>
- [9] F. Brezzi, R. S. Falk, D. L. Marini, Basic principles of mixed virtual element methods, *ESAIM: M2AN* 48 (4) (2014) 1227–1240. doi:10.1051/m2an/2013138.  
URL <http://dx.doi.org/10.1051/m2an/2013138>
- [10] L. Beirão da Veiga, F. Brezzi, L. D. Marini, A. Russo,  $H(\text{div})$  and  $H(\text{curl})$ -conforming VEM, ArXiv e-prints arXiv:1407.6822.
- [11] P. F. Antonietti, L. B. da Veiga, D. Mora, M. Verani, A stream virtual element formulation of the stokes problem on polygonal meshes, *SIAM Journal on Numerical Analysis* 52 (1) (2014) 386–404. arXiv:<http://dx.doi.org/10.1137/13091141X>, doi:10.1137/13091141X.  
URL <http://dx.doi.org/10.1137/13091141X>
- [12] M. F. Benedetto, S. Berrone, S. Pieraccini, S. Scialò, The virtual element method for discrete fracture network simulations, *Computer Methods in Applied Mechanics and Engineering* 280 (0) (2014) 135–156. doi:<http://dx.doi.org/10.1016/j.cma.2014.07.016>.  
URL <http://www.sciencedirect.com/science/article/pii/S0045782514002485>
- [13] L. Beirão da Veiga, F. Brezzi, L. D. Marini, A. Russo, Mixed virtual element methods for general second order elliptic problems on polygonal meshes, *ESAIM: M2AN* 50 (3) (2016) 727–747. doi:10.1051/m2an/2015067.  
URL <http://dx.doi.org/10.1051/m2an/2015067>
- [14] M. F. Benedetto, S. Berrone, A. Borio, S. Pieraccini, S. Scialò, A hybrid mortar virtual element method for discrete fracture network simulations, *Journal of Computational Physics* 306 (2016) 148 – 166. doi:<http://dx.doi.org/10.1016/j.jcp.2015.11.034>.  
URL <http://www.sciencedirect.com/science/article/pii/S0021999115007743>
- [15] A. Fumagalli, E. Keilegavlen, Dual virtual element method for discrete fractures networks, Tech. rep., arXiv:1610.02905 [math.NA] (2016).  
URL <https://arxiv.org/abs/1610.02905>